JAERI-M
7935

JAERI-M 7935

THE ORIGIN OF METAL IMPURITIES IN DIVA

October 1978

K. OHASA, S. SENGOKU, H. MAEDA, H. OHTSUKA,
S. YAMAMOTO, S. KASAI, M. NAGAMI, K. ODAJIMA,
H. KIMURA and Y. SHIMOMURA

日本原子力研究所
Japan Atomic Energy Research Institute

この報告書は，日本原子力研究所がJAERI-Mレポートとして，不定期に刊行している研究報告書です．入手，複製などのお問合わせは，日本原子力研究所技術情報部（茨城県那珂郡東海村）あて，お申しこしください．

JAERI-M reports, issued irregularly, describe the results of research works carried out in JAERI. Inquiries about the availability of reports and their reproduction should be addressed to Division of Technical Information, Japan Atomic Energy Research Institute, Tokai-mura, Naka-gun, Ibaraki-ken, Japan.

JAERI-M 7935

The Origin of Metal Impurities in DIVA

Kazumi OHASA, Seio SENGOKU, Hikosuke MAEDA, Hideo OHTSUKA,
Shin YAMAMOTO, Satoshi KASAI, Masayuki NAGAMI, Kazuo ODAJIMA,
Haruyuki KIMURA and Yasuo SHIMOMURA
Division of Thermonuclear Fusion Research,
Tokai Research Establishment, JAERI

(Received October 2, 1978)

The origin of metal impurities in DIVA (JFT-2a Tokamak) has been studied experimentally. Three processes of metal impurity release from the first wall were identified; i.e. ion sputtering, evaporation, and arcing. Among of these, ion sputtering is the predominant process in the quiet phase of the discharge, which is characterized by no spikes in the loop voltage and no localized heat flux concentrations on the first wall.

"Cones" formation due to the sputtering is observed on the gold protection plate (guard limiter) exposed to about 10,000 discharges by scanning electron micrograph. In the SEM photographs, the spacial distribution of cones on the shell surface due to the ion sputtering coincides with the spacial distribution of intensity of Au-I line radiation. Gold is the dominant metal impurity in DIVA.

The honeycomb structure can decrease release of the metal impurity.

Key Words: DIVA Tokamak, Ion Sputtering, Honeycomb Structure, Metal Impurities, Sputtering Cone, Arcing, Evaporation.

DIVAにおける金属不純物の発生原因

日本原子力研究所東海研究所核融合研究部

大麻　和美・仙石　盛夫・前田　彦祐
大塚　英男・山本　　新・河西　　敏
永見　正幸・小田島一男・木村　晴行
下村　安夫

（１９７８年１０月２日受理）

DIVAにおける金属不純物の発生原因に関する研究の報告である。発生原因としては①イオンによるスパッタリング，②熱の集中による蒸発，③アーキングがあり，特定の条件の下に各々が主原因となっていることを明らかにした。特にプラズマが定常状態にある時には，不純物イオンによるスパッタリングが主原因であることを示した。

実際の装置で使用していたシェル及びProtection plateから切り出したサンプルの表面に，スパッタリングによるcone状の突起が生成されていることをSEM (Scanning Electron Micrograph)を用いることにより観測した。シェル表面のcone状の突起は，Auの発光強度の空間分布と良い一致を示した。更にハニカム構造をもつテストシェルを用いることにより，金属不純物の発生量を減少させ得ることを明らかにした。

CONTENTS

目　　次

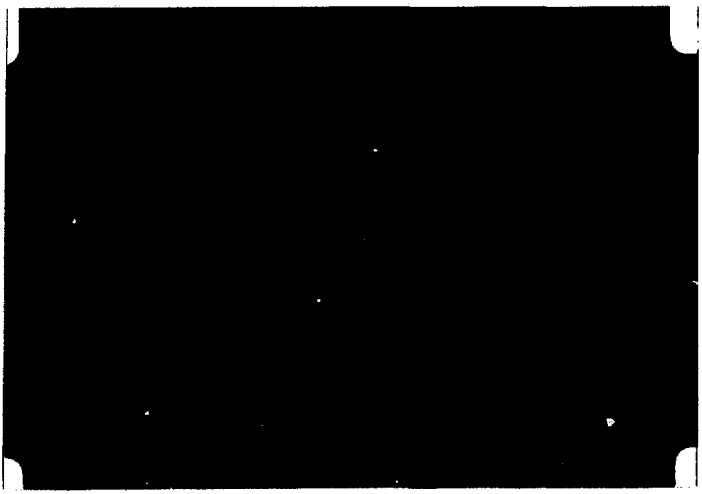

Photo. 1 The cross sectional photograph of the stable diverted tokamak plasma in DIVA taken by using the high speed camera. The exposure time is 250 μs. The left side is the divertor hoop and the right side is the main plasma. The dark point in the right side is the port in the shell.

Photo. 2 The photograph of the unstable plasma. The arc track is clearly observed in the down side of the photograph.

1. Introduction

It is well known that the impurity contamination of the plasma causes an increase in the radiation losses and a decrease of the energy confinement time.[1] Therefore the reduction of the impurity contamination is one of the important problems to be solved to realize the fusion plasma. In the present-day tokamak experiments, impurities are classified into two species, i.e. light impurities (gaseous impurities) and heavy impurities (metal impurities). Many efforts to reduce the light impurities, such as oxygen and carbon, have been done and it has been found that if the first wall surface was made clean by the method of, for example, the flash of titanium[2] or the efficient discharge cleaning,[3] the light impurity contamination could be reduced successfully. However as the light impurity contamination is reduced, the metal impurity contamination increased and the radiation loss due to the metal impurity consumes the main part of the ohmic input power.[4] Therefore the research of the mechanism of the metal impurity release, its contamination in the plasma and the method of the reduction of the metal impurity influx and contamination become more important. J.L. Craston et al. pointed out that the unipolar arcing is the dominant process of the release of the metal impurity in ZETA.[5] G.M. MacCracken et al. also proposed the unipolar arcing as the origin of metal impurities in the DITE Tokamak,[6] however, if the arcing is the dominant process of the release of the metal impurities, it seems difficult to explain rather constant influx of metal impurities as observed in various experiments.[7] It must be pointed out that arcing occurs easily if the reoxidation of the surface is satisfied[8] and there are few works[9] on this problem about the light impurity free plasmas.

In this paper the origin of the metal impurity from the surface contacts to the scrape-off plasma, that is limiter, is described in detail. DIVA can constract the stationary diverted plasma over the whole discharge phase. (Photo. 1) The three processes of the release of metal impurity, that is ion sputtering, evaporation, and arcing, are identified and shown to occur under the different condition of the limiter surface and the potential drop with respect to the plasma. Among these processes, it is made clear that the ion sputtering is the dominant process of the release of the metal impurity from the limiter for the stationary tokamak plasma. Moreover it is demonstrated that the first wall of the honeycomb structure can reduce the metal impurity release from the wall.

2. Experimental Results

The experimental arrangements are shown in Fig. 1. The plasma in the divertor region of DIVA[10] is used to simulate the scrape-off plasma of the conventional tokamak. The parameters of the divertor plasma are as follows; $T_e = 50 - 60$ eV, $T_i = 60 - 80$ eV and $n_e = 2 - 5 \times 10^{12}$ cm ^{3}. An Al target of 6 cm^2 in area located normal to the magnetic field in the divertor simulates the toroidal limiter in the conventional tokamak. The length of the corresponding toroidal limiter is a quarter part of the torus. Aluminium was chosen as the metal impurity because it is not used elsewhere in DIVA and it is clear to decide the position of the impurity source of aluminium. This target is positively or negatively biased with respect to the plasma. At the time when the plasma reaches its stationary state (about 8 ms after the beginning of the discharge), electrical bias is added to the Al target. The time duration of the pulse is 2 ms and this pulse does not cause any change in the marcoscopic discharge characteristics such as the plasma current, loop voltage, plasma density and electron temperature. The voltage of the pulse added between the Al target and the vacuum bessel is changed shot by shot. The probe characteristics of the target, the time evolution of the target current and the time variation of the intensity of Al-III line radiation (3602 Å) are measured. The monochromator is arranged to view directly the target.

The results are shown in Fig. 2 and Fig. 3. In Fig. 2 shows three different types of the time evolution of the intensity of Al-III line radiation and the target current. In Fig. 3 the intensity of the line radiation and the target current are plotted as a function of the applied voltage to the target with respect to the vacuum vessel. From these experimental results, the three different types of the origin of the metal impurity release from the limiter into the plasma are identified as follows.

2.1 Ion Sputtering

As shown in Fig. 3, when the applied voltage to the target is negatively increased, the intensity of the Al-III line radiation continues to increase, whereas the target current saturates at 6 A, that is the level of the ion saturation current. The fact that the target current saturates means the ion flux to the target is constant. But the energy of the colliding ions to the target is increased as increasing the applied voltage. The dependence of the amount of the impurity influx on the energy of the

colliding ion indicates that in this case the impurity release from the target is caused by ion sputtering. The typical time evolution of the intensity of the Al-III line radiation and the target current correspond to the dotted points in Fig. 3 are shown in Fig. 2(a). The time delay in the change of the Al-III line radiation is relatively short as shown and within 200 μs, which corresponds to the characteristic time of the ionization and excitation of the aluminium to the state of this radiation in the divertor plasma. The short time delay of the release of the aluminium from the target and the time independent impurity influx into the plasma also indicates that the mechanism of the release is not the thermal process but the atomic process, i.e. ion sputtering. Moreover, as shown by the solid line in Fig. 2(c), when the floated target is biased positively to retard the ion, the intensity of the line radiation of aluminium is decreased to the level without the target if the pulse duration is short and the heat flux is small enough.

The damage due to the ion sputtering is too microscopic and can not be observed on the target surface desposed to the plasma over only a few hundred discharges. But the cone like formations due to the ion sputtering can be observed on the surface of the gold protection plate (guard limiter attached to the shell) desposed to the plasma over 10000 discharges (Fig. 4) This picture is taken using the scanning electron micrograph (SEM) technique. The cone like formations are clearly observed in the region some distance apart from the edge of the protection plate, although the cones in the edge region are destroied by the damage due to the evaporation and/or arcing. This picture shows clearly that the ion sputtering really occurs on the first wall surface of the real tokamak machine.

2.2 Arcing

As shown in Fig. 3 by the crossed points, the large target current is observed. The time evolution of the target current and the intensity of Al-III line radiation is shown in Fig. 2(b). This class of the release of the metal impurity is obviously distinguished from the class of ion sputtering described above. As shown in Fig. 3, the target current is 40 A, that is larger than the ion saturation current by the factor of ten, and increased as the applied voltage increased. The larger target current indicates that the mechanism of the release of the metal impurity for this class is arcing as pointed by R. Hancox et al.. The arcing is observed only in the first about ten shots after inserting the target into the

divertor plasma. This indicates the conditioning effects widely observed in discharge phenomena and also suggests that the process of this type of impurity release corresponds to arcing. Aluminum is the material that the arcing is easily occurred. A one-shot-exposed target, where the target is electrically floated, indicates clear arc tracks (Fig. 5) as observed in DITE. It must be noted that the arc tracks are observed on the target surface in both sides, i.e. the side of ion flow and the side of electron flow. Therefore the arcing does not caused by the runaway electrons.

2.3 Evaporation

As shown in Fig. 2(c), when the target is positively biased and collects electron currents, the intensity of the Al line radiation is increased with the time delay of 1-2 ms. The electron current is greater than the ion saturation current by the factor of ten. In this case the heat flux to the target is greater than the case with positive biase. The time delay of 1-2 ms of the impurity release corresponds to the characteristic time of the aluminium target to melt. These results suggest that the mechanism of the release of the metal impurity in this class is evaporation due to the heat flux by the electron.

It is only when the electrically floated target is so placed to accept high energy electrons from the main plasma that the SEM picture of the target surface indicates many melted spots (Fig. 6) in the present experiments. In this case the target may be evaporated due to the concentrated heat flux of runaway electrons.

3. Discussions

3.1 Origin of Metal Impurities

Observed processes occur under the different electrical and surface conditions of the target. The target in this experiment simulates the limiter in tokamak discharges.

The limiter is sometimes used as grounded or as floated electrically in conventional tokamak. Arcing occurs only when the limiter has negative potential to the scrape-off plasma, but can be easily suppressed by discharge cleaning of the limiter surface as shown in the present experiments. Arc tracks, however, are observed on the surface of a one-shot-exposed

target which is electrically floated. Arcing may occur when the negative spikes appear. By using a high speed camera, several lighting due to arcing are clealy observed on a shell surface in the disruptive plasma discharge (Photo. 2). The arcing on the shell is occurred only in this discharge during over 50 discharges observing by the high speed camera. Evaporation may occur when the heat flux to the limiter is increased to the level about ten times greater than the normal heat flux by the stationary plasma. Although these processes may occur under the special condition of the plasma and the limiter surface, they do not occur when the plasma becomes its stationary state. The experimental results described above indicate that the ion sputtering is the dominant process of the release of the metal impurity from the limiter contacting to the quasi-stationary scrape-off plasma in tokamak.

In Fig. 7 the intensity of the line radiation, that correlates to the quantity of the metal impurity efflux by ion sputtering, is plotted as a function of the applied voltage to the target. The intensity of Al-III line radiation, and the Au-I line radiation when the shell coated by gold is biased, are also plotted in the same manner. These results suggest that when the accelerating potential is below 400 V, the main part of the ion sputtering may be caused by the impurity ions and above 400 V, the ion sputtering by the hydrogen may become dominant, because the energy gained by the ion of charge Z is Z-times greater than the energy gained by the hydrogen. On this point of view, the sputtering yields of H^+, Au and Ne on Au are shown in Fig. 8. Data are taken from the reference 11. Unfortunately, data on oxygen are not available and neon is shown for an example to see the rough dependence of sputtering yield of oxygen on Au. These traces are obtained assuming the effective charge $\bar{Z}$ of Au and Ne are 10 and 3, which values are probably true in the present scrape-off plasma parameters. The horizontal axis for Au and Ne are divided by $\bar{Z}$ because the energy of these impurity incident fluxes to the target is $\bar{Z}$ times the potential difference between the plasma and the target. These traces remarkably resemble the experimental results on Au obtained by biasing the shell coated by gold, in which there are two threshold energies, i.e. a few hundreds eV and a few tens eV. It is difficult to estimate the fluxes of Au and Oxygen onto the shell surface experimentally. However, the pseudo-continuum emission did not change when the oxygen concentration was reduced by a factor of 2 with the titanium gettering. Therefore the self-sputtering of gold is responsible for the observed ion sputtering.

The spacial relation between the metal impurity efflux and the damage on the shell surface due to the ion sputtering is studied.

Fig. 9 shows the spacial intensity distribution of the Au-I line radiation and the scanning electron micrograph pictures of various area of the shell coated with gold. The shell is disposed to the plasma over a few ten thousands discharges. There is also the picture of the shell surface before the disposure to compare with the photographs after the desposure. The surface is created by the ion plating method[12]. The cone like formations due to the ion sputtering is more clearly observed in the area of throat, i.e. the left side of the figure. It corresponds to the area of the maximum intensity of Au-I line radiation. Gold is the dominant metal impurity in DIVA. There is a fairly good correlation between the area of the maximum intensity of the metal line radiation and the area of the maximum growth of the cone like formations due to the ion sputtering. It indicates that the ion sputtering is the dominant process of the metal impurity release from the first wall in DIVA.

From these considerations, it can be said that the high-Z impurity ion sputtering must be dominant when the sheath potential is as low as in the usual scrape-off plasma, i.e. $\phi \sim 150 \sim 200$ V. The contribution of the sputtering by the neutral atoms to the metal impurity contamination is concluded to be very little because of the electrical potential dependence on the metal impurity release.

3.2 Effectiveness of Honeycomb Structure as a Neutralizer Plate

It is well known that honeycomb structure successfully reduces the metal efflux from the surface against the bombardment of high energetic neutral particles.[13] Therefore if the ion sputtering is the dominant process for the metal impurity efflux, the surface of the honeycomb structure reduces the metal impurity efflux. In the present experiments the plane target is replaced by the honeycomb target (Fig. 10) and the comparison of the metal efflux with the plane target is performed. In Fig. 11 the efflux of Al vs. applied voltage to the honeycomb target is shown, comparing to those of the plane target. This result shows that 30 - 40 % of the metal efflux is reduced by employing a honeycomb structure as a neutralizer plate. According to the calculation[14], in which the sputtered metal is free from ionization and travels straight from the surface as a neutral particle, the reduction must be 70 - 80 %. The discrepancy between the observed and the calculated values may be explained

by taking into account the ionization of the sputtered atoms in the scrape-off plasma in front of the honeycomb target. Figure 12 shows the trapping efficiency of the honeycomb structure as a function of a mean free path λ of the sputtered atom.

It is difficult to determine the mean free path of the sputtered aluminum atoms experimentally, however, some crude estimation can be given as following. Assuming the energy of the sputtered aluminum atoms to be some reasonable value of 3 eV and using the ionization rate coefficient in the present scrape-off plasma parameters ($n_e = 2-5 \times 10^{12}$ cm^{-3}, $T_e = 40-60$ eV), the mean free path λ is calculated to 7 mm. Because of this finite λ, the trapping efficiency is reduced from 80 % to 45 % and is consistent with the experimental results. This result shows that the size of a honeycomb has to be small not only because of thermal problems but also because of ionization processes. This experiment suggests that the honeycomb structure is also as effective in reducing metal effluxes from a neutralizer plate as in reducing them from the first wall surrounding the main plasma.

Since gold has a high sputtering yield and a poor thermal property, plasma-wall interactions in DIVA simulates those in a higher temperature scrape-off plasma in a large machine with a suitable wall material. For example, sputtering yield for gold contacting to a 50 eV hydrogen plasma has the same value of that for molybdenum contacting to a 200 eV hydrogen plasma.

4. Conclusion

It is experimentally demonstrated that in the stationary-phase discharge without negative spikes, ion sputtering is the dominant process of the release of the metal impurities from the limiter or the neutralizer plate in tokamaks, and that the honeycomb structure employed as the neutralizer plate reduces 30 - 40 % of the metal efflux from the surface even though the ionization of the sputtered atoms in the scrape-off plasma reduces the trapping efficiency of the honeycomb structure. The present experimental results show that it is important to decrease the energy of the ion that sputters to the limiter in order to reduce the metal impurity contamination in the present tokamak plasma. The energy of the sputtering ion accelerated by the sheath potential can be decreased if the plasma temperature of the scrape-off layer is decreased. Therefore the control

of the scrape-off plasma is the important techniques to avoid the metal impurity contamination[15]. There is an important experimental result, that is, the metal impurity efflux decreases when the light impurity efflux increases[16]. The reduction of the metal impurity efflux is due to the cooling of the scrape-off plasma by the radiation loss of the light impurity, The cooling induces the reduction of the sheath potential and reduces the metal impurity release due to the ion sputtering.

Acknowledgement

We are grateful to members of DIVA operation-group for their assistance in the experiment. Drs. S. Mori, M. Yoshikawa, Y. Obata M. Tanaka and Y. Tanaka are gratefully acknowledged for their containuous encouragements of our work.

References

1) C. Breton et al., Nucl. Fusion 16 (1976) 891
R.V. Jensen, D.E. Post, D.L. Jassby, Princeton Plasma Physics Laboratory Report PPPL-1350 (1977)
T. Tazima et al., Nucl. Fusion 17 (1977) 419

2) P.E. Stott, C.C. Daughney and R.A. Ellis, Nucl. Fusion 15 (1975) 431

3) L. Oren, R. Taylor, University of California Report PPG-294 (1977)

4) L.A. Berry et al., in Proc. of 6th Conf. on Plasma Phys. and Controlled Nuclear Fusion, Berchtesgaden (1976) Paper IAEA-CN-35/A4-1
E.B. Meservey et al., Nucl. Fusion 16 (1976) 593

5) J.L. Craston et al., in Proc. of 2nd U.N. Conf. on Peaceful Uses of Atomic Energy, Geneve (1958) 414

6) G.M. MacCracken et al., in Proc. of 8th European Conf. on Controlled Fusion and Plasma Physics, Prague, vol.I (1977) 40

7) TFR Group, Fontenay-Aux-Roses Report EUR-CEA-FC-868 (1977)
E. Hinnov and M. Mattioli, Princeton Plasma Physics Laboratory Report PPPL-1375 (1977)

8) R. Hancox, British Journal of Applied Physics 11 (1960) 468
A.E. Guile, in Proc. IEE, IEE Reviews 118 (1971) 1131

9) K. Ohasa et al., Nucl. Fusion 18 (1978) 872

10) S. Yamamoto et al., in Proc. of 8th European Conf. on Controlled Fusion and Plasma Physics, Prague, vol.I (1977) 33

11) $H^+ \rightarrow$ Au
H.L. Bay, J. Roth and J. Bohdansky, J. Appl. Phys. 48 (1977) 4722
Ne → Au
N. Laegreid and G.K. Wehner, J. Appl. Phys. 32 (1961) 365
D. Rosenberg and G.K. Wehner, J. Appl. Phys. 33 (1962) 1842
Au → Au
W.H. Hayward and A.R. Wolter, J. Appl. Phys. 40 (1969) 2911
O. Almén and G. Bruee, Nucl. Instr. & Meth. 11 (1961) 279

12) S. Komiya, M. Mizuno, T. Narusawa, H. Maeda, and M. Yoshikawa, Japan. J. Appl. Phys. Suppl. 2, Pt.1, (1974) 363

13) K. Obara, S. Abe, H. Nakamura, Japan Atomic Energy Research Institute Report JAERI-M 7216 (1977)

14) M. Yoshikawa, Japan Atomic Energy Research Institute Report JAERI-M 5849 (1974)
S.N. Cramer and E.M. Oblow, Nucl. Fusion 15 (1975) 339

15) Y. Shimomura, Nucl. Fusion 17 (1977) 626

16) M. Nagami, H. Maeda, T. Yamauchi, S. Sengoku, S. Kasai, T. Sugie, H. Kimura, K. Ohasa, K. Odajima, S. Yamamoto, Y. Shimomura, to be published in Suppl. J. Nucl. Material.

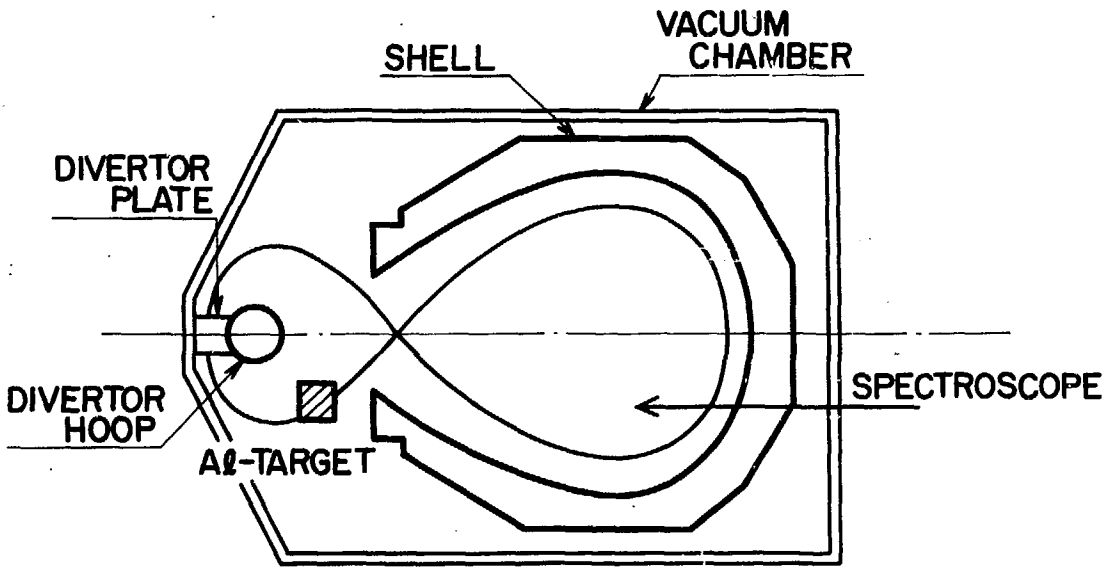

Fig. 1 Schematic of the experimental setup

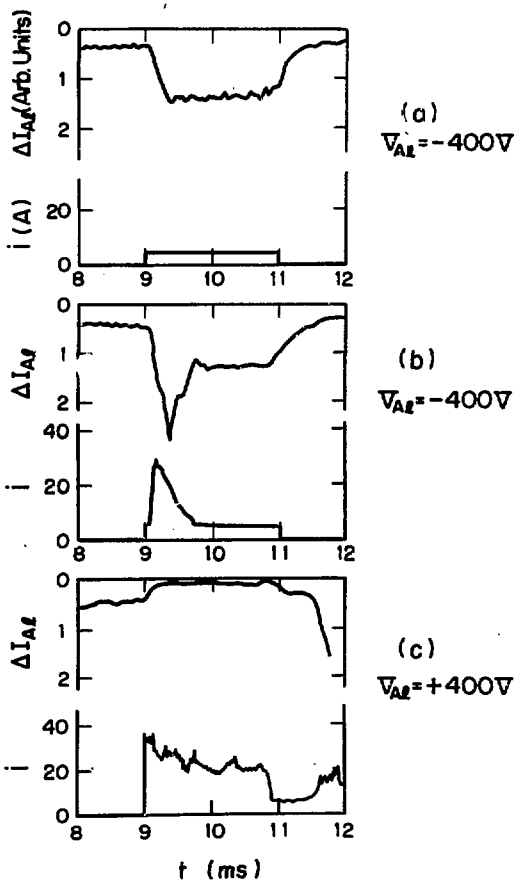

Fig. 2 Typical time evolutions of the intensity of Al-III line radiation (3602 Å) and the probe current. The target is biased from 9 ms to 11 ms. The applied voltage of the pulse is shown. Each graph shows (a) Ion Sputtering, (b) Arcing, (c) Evaporation, respectively.

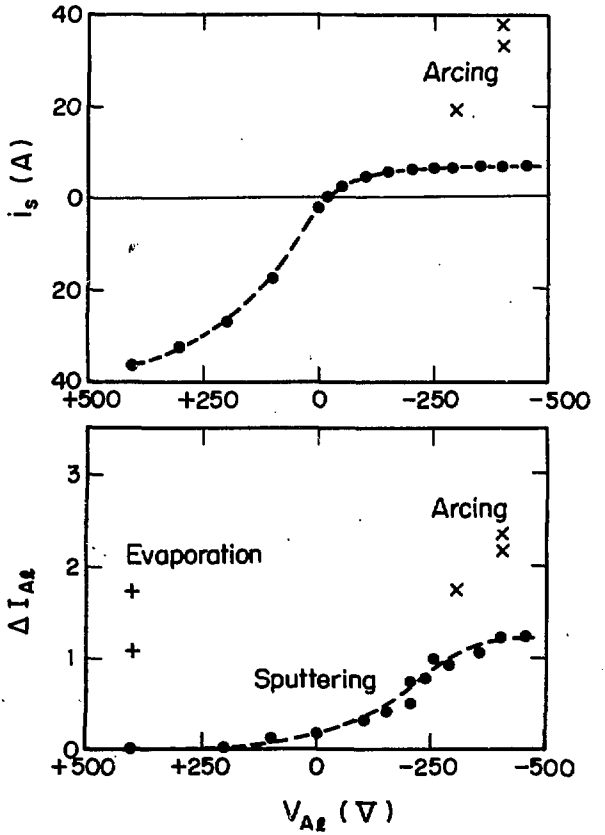

Fig. 3 The dependence of the probe current and the intensity of the Al-III line radiation on the applied voltage to the Al-target. The experimental results are classed clearly into the three types. Closed circles correspond to the type (a) in Fig. 2, i.e. Ion Sputtering. Crossed points correspond to the type (b) in Fig. 2, i.e. Arcing. Dagger points correspond to the type (c) in Fig. 2, i.e. Evaporation.

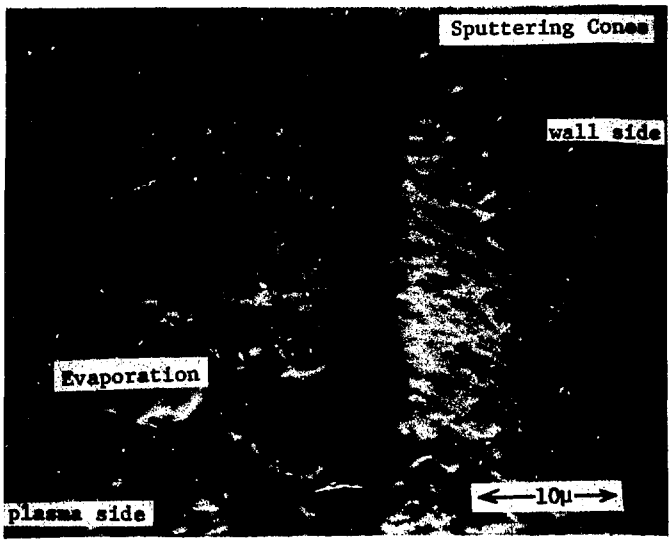

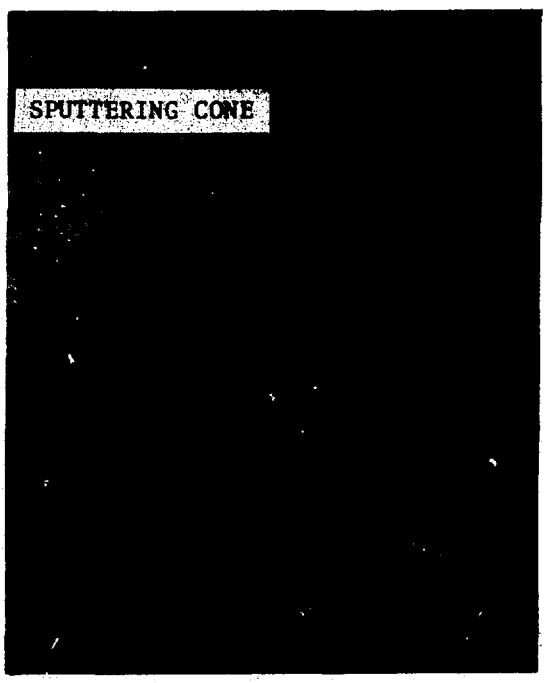

Fig. 4 The scanning electron micrograph picture of a gold protection plate surface. The cone like formation due to the ion sputtering are observed. The protection plate was desposed to the plasma about 10000 discharges.

Fig. 5 Scanning electron micrographs of arc tracks on the electrically floated aluminum target located in a divertor.

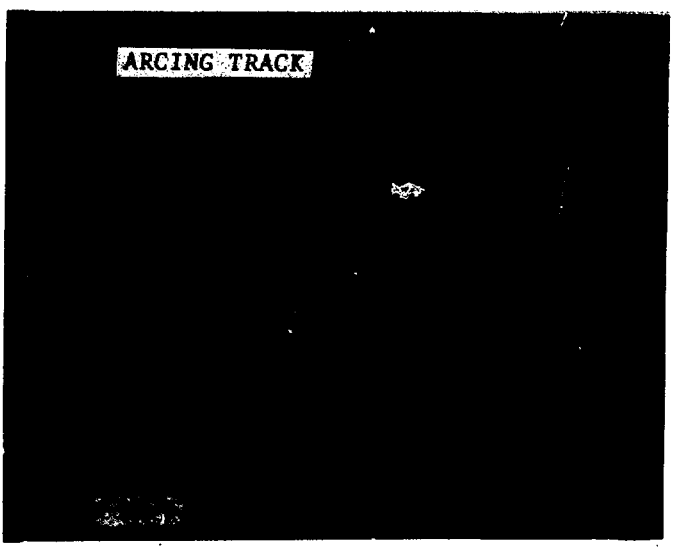

Fig. 6 Scanning electron micrographs of the many melted spots on the electrically floated aluminum target in a divertor. These spots are created by high energy electrons from the main plasma.

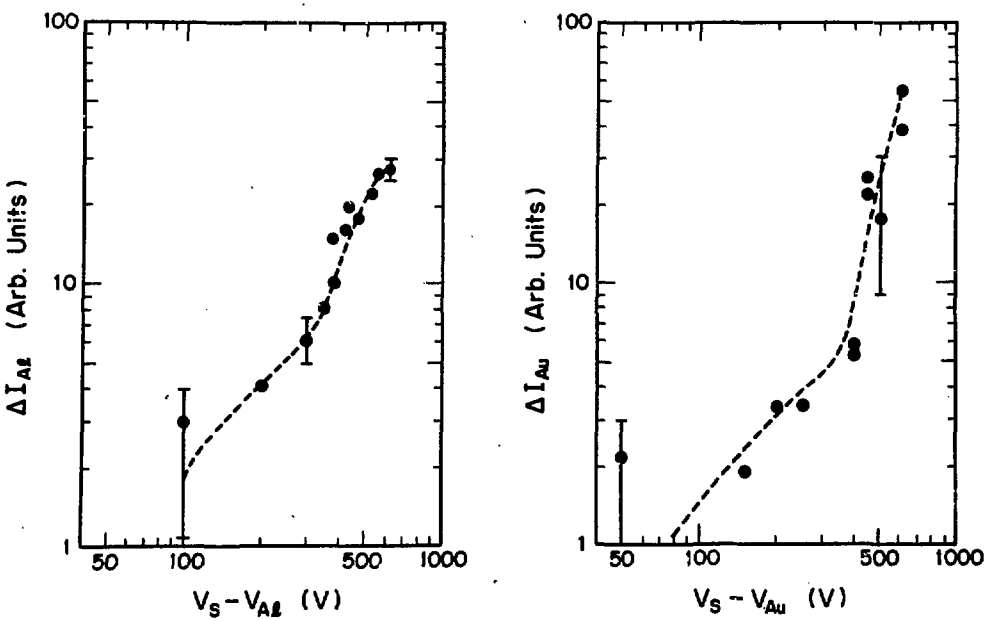

Fig. 7 Dependence of the intensity of Al-III and Au-I line radiation in the case of (a) in Fig. 2 on the applied voltage to the Al-target or the gold plated shell. V_S-V_{Al} means the potential gap between the plasma space potential and the Al-target. V_S-V_{Au} means the potential gap between the plasma space potential and the gold plated shell.

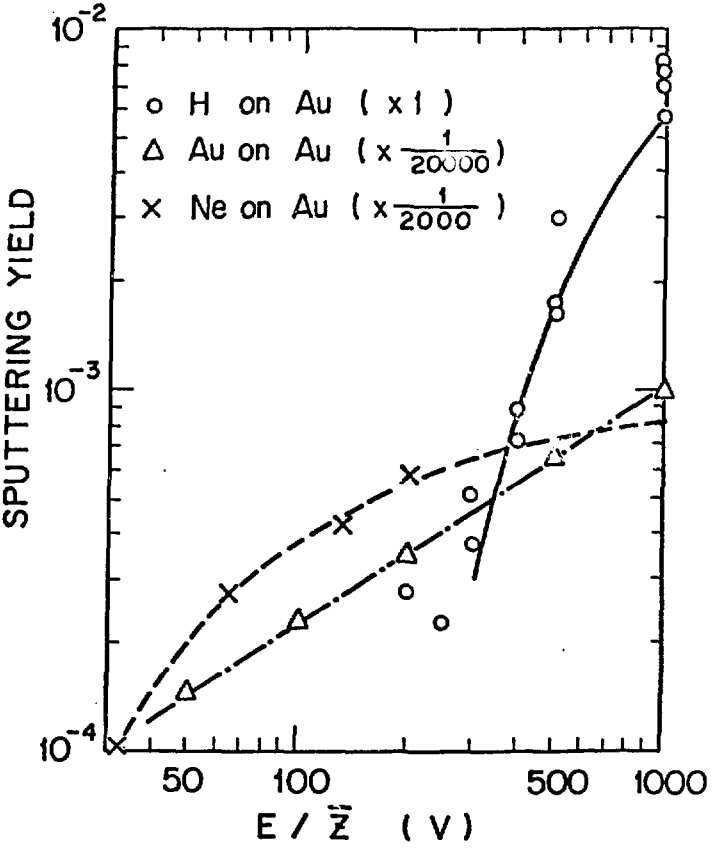

Fig. 8 Sputtering yields of H^+, Au and Ne on Au taken from reference 11.

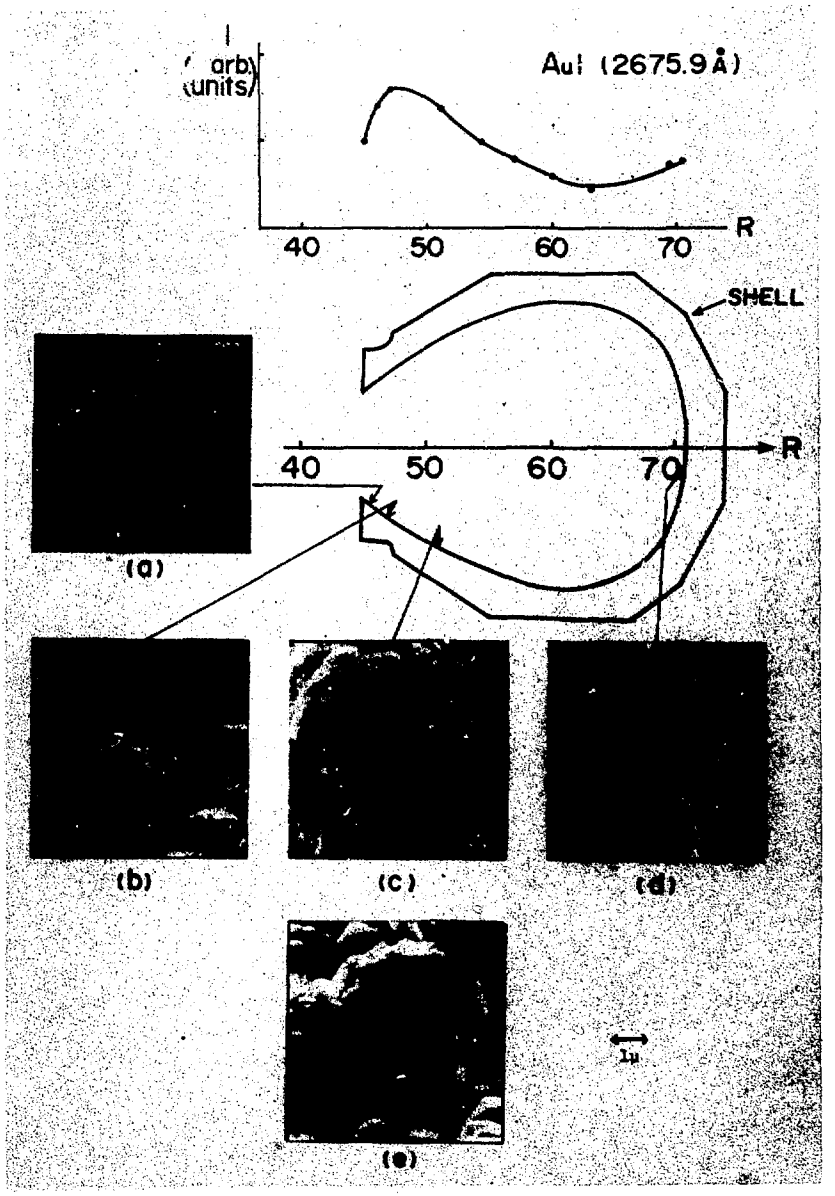

Fig. 9 (a)-(d) The SEM pictures showing the cone like formations due to the ion sputtering in the various area of the shell surface.
(e) The SEM pictures of the surface before the desposure to the plasma. The shell surface coated with gold is created by the method of ion platting.
The radial distribution of the intensity of the Au-I line radiation is also shown.

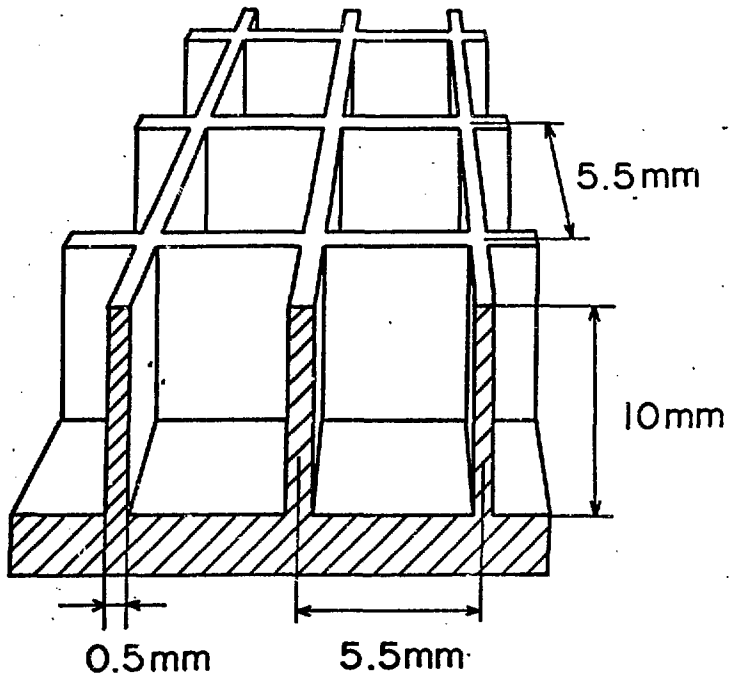

Fig.10 Schematic drawing of a honeycomb target.

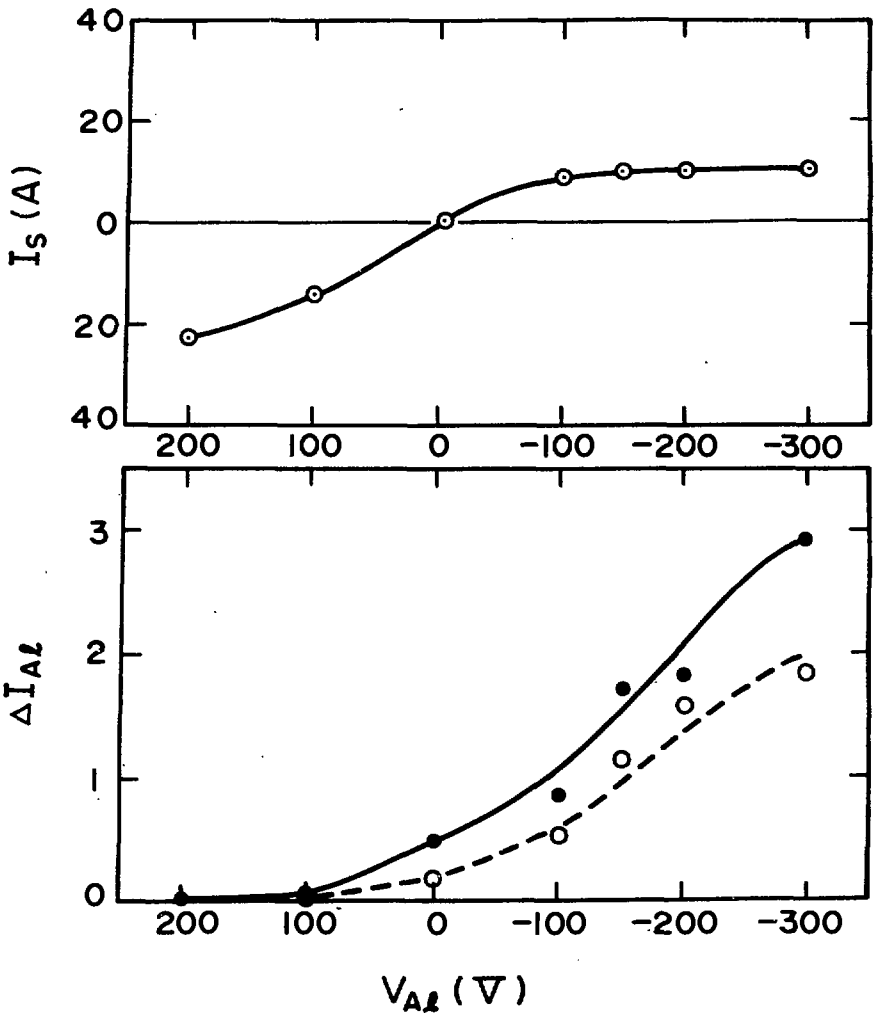

Fig.11 Efflux of aluminum from the honeycomb target. Open circles correspond to the honeycomb target and closed circles correspond to the plane target. The top trace shows the target current vs. applied voltage to the target.
The bottom trace shows the efflux of aluminum vs. applied voltage to the target.

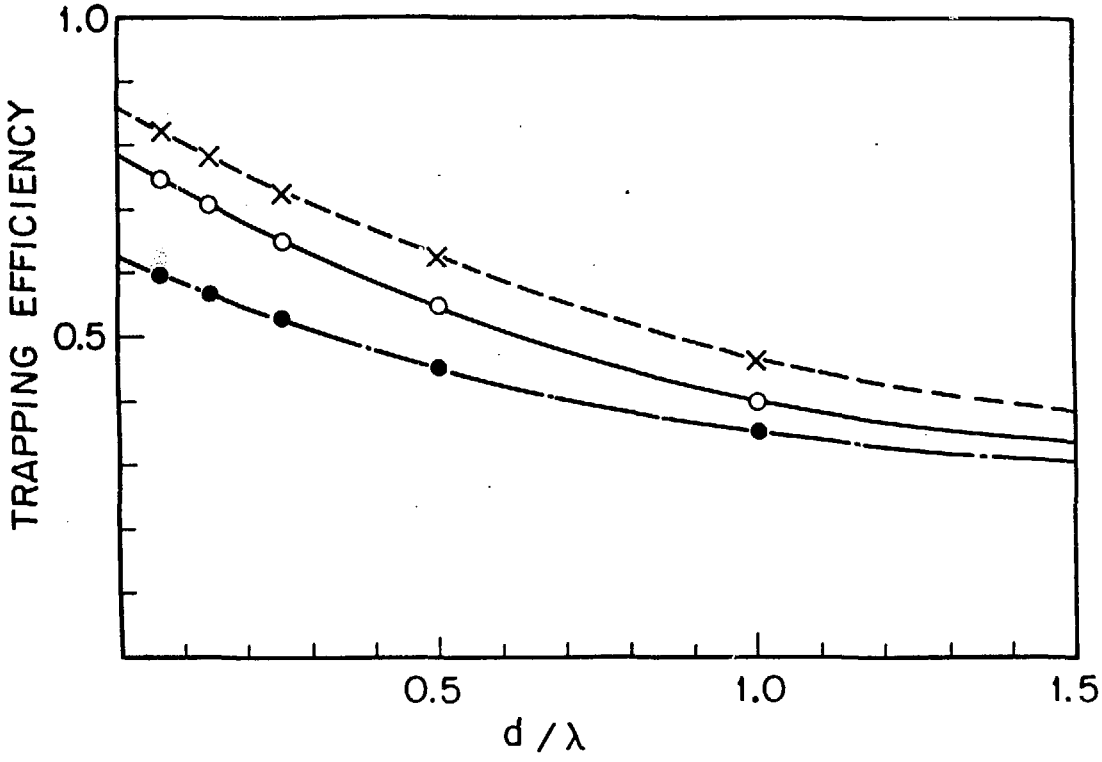

Fig.12 Trapping efficiency of the honeycomb structure as a function of the mean free path λ of the sputtered neutral atom calcualted using the Monte Calro Method. D is the depth of the honeycomb and d is the width of the honeycomb. Angular distribution of the sputtered atom is assumed to be cosine distribution (open and closed circles). The case of homogeneous distribution is also calculated and shown by the crossed points. D/d = 1.0 for closed circles and D/d = 2.0 for open circles and crossed points.